Experiment and Simulation of Reflected Slow and Fast Wave Correlation with Cancellous Bone Models

Muhamad Amin Abd Wahab[1]
[1]School of Electrical Engineering,
Faculty of Engineering,
81310 Johor Bahru, Malaysia.
mamin55@liveutm.onmicrosoft.com

Rubita Sudirman[1]
[1]School of Electrical Engineering,
Faculty of Engineering,
81310 Johor Bahru, Malaysia.
rubita@fke.utm.my

Mohd Azhar Abdul Razak[1]
[1]School of Electrical Engineering,
Faculty of Engineering,
81310 Johor Bahru, Malaysia.
mohdazhar@fke.utm.my

Nasrul Humaimi Mahmood[1]
[1]School of Electrical Engineering,
Faculty of Engineering,
81310 Johor Bahru, Malaysia.
nasrulhumaimi@fke.utm.my

Abstract— **Incorporating fast and slow wave analysis into ultrasound measurements can improve the accuracy of bone quality estimation to detect the risk of osteoporosis-related fractures. Since the pulse-echo technique can perform measurements at critical bone locations, this technique is offered by applying fast and slow wave analysis to improve the accuracy of the measurement technique. Thus, the objective of this paper is to conduct simulation and experiment for the pulse-echo technique to investigate correlation reflected fast and slow wave with various porosity of cancellous bone models. The recorded reflected wave (mix wave) is separated method into individual reflected fast and slow wave using bandlimited deconvolution. Further, the parameters for the mix, fast and slow waves are calculated, plotted against porosity and correlation of the parameter's data is observed. The result between simulation and experiment also compared in terms of parameters behaviour versus porosity. The result shows that the reflected fast and slow wave separated using bandlimited deconvolution method has characteristics that represent wave that propagate through solid or pore part of the porous structure as found by previous works. Moreover, the simulation result shows that the parameter of reflected fast and slow wave shows a high correlation with porosity. However, for experiment, only attenuation parameters shows significant correlation with porosity (R^2_{fast} = 0.51 and R^2_{slow} = - 0.76). The experiment may experience additional undesired noise in comparison with the simulation. Nevertheless, the attenuation parameters were consistent between the simulation and the experiment. The overall result shows that studying fast and slow waves instead of mix waves for bone quality estimation can help improve the accuracy of pulse-echo measurement.**

Keywords—bandlimited deconvolution, fast and slow wave, polyurethane, pulse-echo, ultrasound

I. INTRODUCTION

Ultrasound systems are widely used in many applications such as in engineering, medicine [1], biology, and other areas [2]. Ultrasound propagation through a porous structure has been shown to accommodate two types of longitudinal waves, namely fast and slow waves. These two waves also demonstrate a high correlation with the cancellous bone microstructure. [3-9]. This finding may offer another way to improve bone quality assessment using ultrasound to diagnose bone loss due to osteoporosis. However, these two modes waves often interfere with each
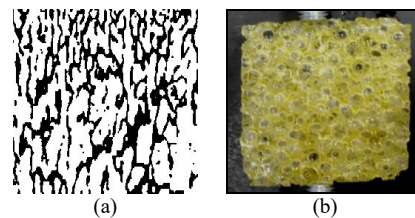

Fig. 1. (a) Example of 2-D cancellous models with porosity level of 66% and (b) PU foam Sawbones® samples with porosity of 90%

other due to a high degree of cancellous bone anisotropy [10]. As a result, many methods have been developed to distinguish fast and slow waves, and some of them are the Bayesian and Modified Prony's method [11-15]. Among the wave separation methods, the bandlimited deconvolution is selected because it is simple to implement and does not require the initial assumption of transmission parameters [14, 15]. One of the techniques to measure ultrasound waves is pulse-echo (PE), and this technique uses only a single transducer which makes it capable of measuring at the skeletal site of life such as the hip and spine. However, due to the complicated conduct of the reflected and backscattered wave relationship with the inhomogeneity of cancellous bone, the precision of the PE technique is still not powerful compared to the transmission (TT) technique. As a result, Hosokawa [3, 16-18] has performed Finite Difference Time Domain (FDTD) simulation to demonstrate that fast and slow waves can also be reflected and backscattered and from this discovery, the two modes waves might become an alternative approach to improve the accuracy of the PE technique for estimating bone quality.

Therefore, the purpose of this study was to perform a 2-Dimensional (2-D) simulation and experiment using PE technique to provide an alternative method to obtain a fast and slow reflected wave and to investigate the connection of those waves with different porosities of cancellous and bone phantom models. The reflected fast and slow wave will be separated from the reflected wave (mix wave) by using the bandlimited deconvolution method. Then, the correlation coefficient of ultrasound parameters versus porosities will be contrasted between single-mode (mix), fast and slow waves. Moreover, the outcome for both simulation and

experiment also compared in terms of ultrasound parameters behaviour versus porosity.

II. MATERIAL AND METHOD

A. 2-Dimentional Cancellous Models

The 2-D cancellous model is a model of cancellous bone from previous works by Gilbert *et al.* [19]. In particular, there are 9 cancellous models with porosity levels ranging from 30 % to 7 5% for the simulation.

TABLE I.   MATERIALS PROPERTIES FOR THE SIMULATION AND EXPERIMENT.

No.	Material	ρ (g/cm³)	Simulation		Experiment (PU foam)	
			ϕ	v (m/s)	ϕ	Cell size (mm)
1.	Water	1000	-	Cl: 1497 Cs: 0	-	-
2.	PU	1100	0.30 – 0.75	Cl: 1700 Cs: 697	0.73 – 0.90	0.50 – 1.00

ϕ: Porosity, ρ: Density, v: Velocity, *Cl*: Longitudinal Velocity, *Cs*: Shear Velocity

The scale of the 2-D cancellous model image geometric scenario is 170 × 125 pixels and 25 pixels / mm was set in the simulation. The porosity values measured by ImageJ software based on a color threshold between black and white colour. The thickness of the cancellous models is 8 mm. An example of 2-D cancellous models for the simulation is shown in Fig. 1 (a), where black colours represent solids and white colours represent liquids (water).

B. Simulation Setup for Pulse-Echo Measurement Technique

SimNDT version 0.43 is the programme used for this investigation [20]. The simulation setup was based on PE measurement technique with a 1 MHz single Gaussian sine wave as the output pulse for the transducer. Referring to Fig. 2 (a), the transducer was a planar type with a size of 5.5 mm. The air-water boundary below the cancellous models will act as a reflector element to reflect the ultrasound wave to the transducer. The simulation time was set to 40 μs and the pulse of the input voltage was set to 20 volts peak-to-peak (V_{pp}). The distance between the transducer and bone models is 8 mm. An absorbing layer with a thickness of 5 mm surrounded the simulation area. Table 1 (Simulation) show the acoustic and material properties of PU and water-based on acoustic properties database from the signal-processing website [21]. The parameter's value such as density and velocity in Table 1 also set in the simulation to represent the type of material used, e.g., density = 1 kg/cm³, $Cl = 1497$ m/s and $Cs = 0$ m/s represent water substance.

C. Rigid Polyurethane foam

Bone phantom (Rigid Polyurethane (PU) foam, Sawbones[®]) was the samples used to surrogate the actual cancellous bone for the experiment. The stress-strain curve, cell size and microstructure of these PU foams are comparable to real cancellous bone [22, 23]. An example of PU foam, Sawbones[®] for the experiment, is shown in Fig. 1 (b). There are five (5) types of PU foam used for this
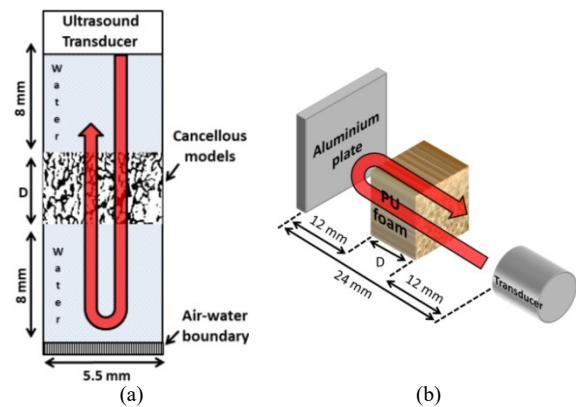

Fig. 2. (a) Simulation and (b) experiment setup diagram for PE measurement technique

experiment, as shown in Table 1 (experiment), with porosity values varying from 73 % to 90 %. Although only five (5) samples of PU foam, the range of the porosity value are sufficient to represent healthy and unhealthy cancellous bone [24]. Also, the thickness of the PU foam is 8 mm. For at least 24 hours before the experiment began, the PU foam was immersed in water to ensure that the water is filled in the pore space of the foam, as usually done by previous researchers [7].

D. Experiment Setup for Pulse-Echo Measurement Technique

The PE measurement technique uses only one transducer to operate and act as both the transducer and receiver. Besides, the aluminium plate was used to reflect the wave to the transducer. The distance between the transducers with the aluminium plate for PE technique was 24 mm with PU foam was located 12 mm between them as demonstrated in Fig. 1 (b). A pulser/receiver (5077PR, Panametrics, Olympus) was used as a signal generator. The ultrasound transducer used was a broadband type with 1 MHz in centre frequency, 13 cm in diameter and 1.5 cm of focal length. The experiment was conducted in a clear tank filled with water. For the signal source, the input voltage was set to 300 V_{pp} with a gain of 25 dB. The received signals digitized using an oscilloscope (Tektronix digital oscilloscope), stored on a computer via general-purpose interface bus (USB) and analyzed using Mathlab software. Measurements were conducted several times, and for each measurement taken, about 64 signals were averaged.

E. Bandlimited Deconvolution method

The bandlimited deconvolution is a method to separate mix wave or single-mode wave into an individual fast and slow wave [14, 15]. The basis of the bandlimited deconvolution method is based on Eq. 1 developed by Marutyan *et al.* [25] as a mathematical model for the propagation of ultrasound waves through the porous structure.

$$Y(f)=X(f)[Hfast(f)+Hslow(f)] \qquad (1)$$

$X(f)$ is the spectrum of the wave passing through water only (reference wave) while $Y(f)$ is the spectrum of the wave passing through a sample (mix wave). *f* is the ultrasound
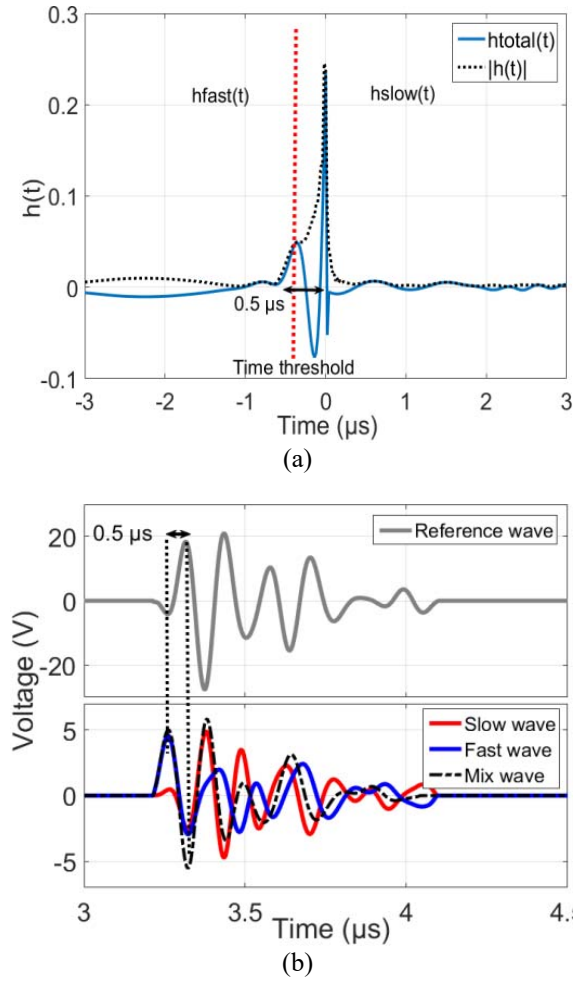
(a)

(b)

Fig. 3. Examples of (a) transfer function and (b) reflected fast and slow wave in the time domain of PU foam for the experiment (porosity = 86%).
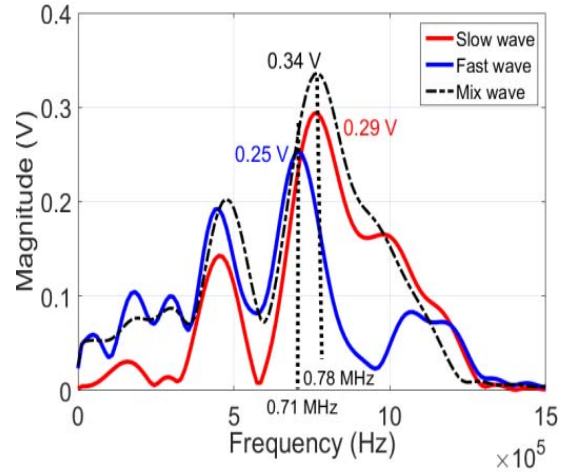

Fig. 4. Amplitude (*A*) spectrum of the reflected fast, slow and mix waves of PU foam for the (porosity = 86%).

where *D* is the sample thickness in cm, *SR(f)* is the amplitude spectrum of a reference wave and *SB(f)* is the amplitude spectrum of the sample wave. The *β(f)* slope frequency range would be from 0.2 to 0.6 MHz with the unit of dB/cm/MHz. For the signal loss parameters, the formula to calculated are as follow [29],

$$SL=20 \log 10 [SR(f) / (SB(f)]\qquad(3)$$

where *SR(f)* is the amplitude spectrum of a reference wave, and *SB(f)* is the amplitude spectrum of the sample wave. The unit of the signal loss is in decibel (dB) and the value is taken at the 1 MHz frequency of the broadband signal.

III. RESULT AND DISCUSSION

A. Separation of reflected wave

Fig. 3 (a) shows an example of the transfer function of reflected mix wave, *htotal(t)*. The red dash line represents a time threshold that divided *htotal(t)* into *hfast(t)* and *hslow(t)*. Based on the reflected reference wave arrival time (i.e., time = 0), time threshold was set roughly at the time of − 0.25 µs (the time threshold was set 0.25 µs earlier compare to the reference reflected wave arrival time). Time threshold was also set based on the wave envelope, |*h(t)*| (black dash line) to assumed the boundary between the estimated fast and slow wave. The sign of the two modes waves can be seen, where two "peaks" have been observed in Fig. 3 (a). The first "peak" is located at the time of 0 µs (indicate almost the same velocity with reference wave) and presumed as *hslow(t)*. This is because the velocity of the slow wave is typically in ranges or slower relative to the reference wave (1479 m/s), which is about 1150 to 1452 m/s, as previous researchers found [7, 24]. Meanwhile, another smaller "peak" is located roughly at the time of − 0.5 µs and presumed as *hfast(t)*.

The left side region of the time threshold is multiplied with rectangular time-domain window with a value of one while the right side region is multiplied with zero. The output for this computation is assumed as the transfer function of fast wave, *hfast(t)*. Then, *yfast(t)* and *yslow(t)* are computed and obtained as explained previously in the bandlimited deconvolution method section. Referring to Fig.

frequency. An element in the brackets of the Eq. 1 represents a coefficient of transmission. The transfer function, *Hfast(f)* and *Hslow(f)* for the porous structure were considered to be two waves propagating simultaneously through the linear-with-frequency attenuating medium. [26]. The bandlimited deconvolution method estimate transfer function of fast wave, *hfast(t)* based on the velocity above 1479 m/s = reference wave. As the name suggests, the fast wave is predicted to be faster than the reference wave. Based on the Eq. 1, *hfast(t)* then computed by using FFT into *hfast(f)* and multiply with *X(f)* and becoming *Yfast(f)*. After that, the fast wave in the time domain, *yfast(t)* is obtained by computed IFFT to the *Yfast(f)*. To obtain slow wave in the time domain, *yslow(t)*, the mix wave in the time domain, *y(t)* subtracted the *yfast(t)*. More information on the method can be found in previous works [14, 27, 28].

F. Ultrasound Wave Parameter

The ultrasound parameters involved in this investigation were amplitude (*A*), frequency-dependent attenuation (*β*) and signal loss (*SL*). The amplitude parameter was the value obtained at the peak value of signal magnitude in the frequency domain with a unit of V. The measurement formula for the attenuation parameter is as follows [14],

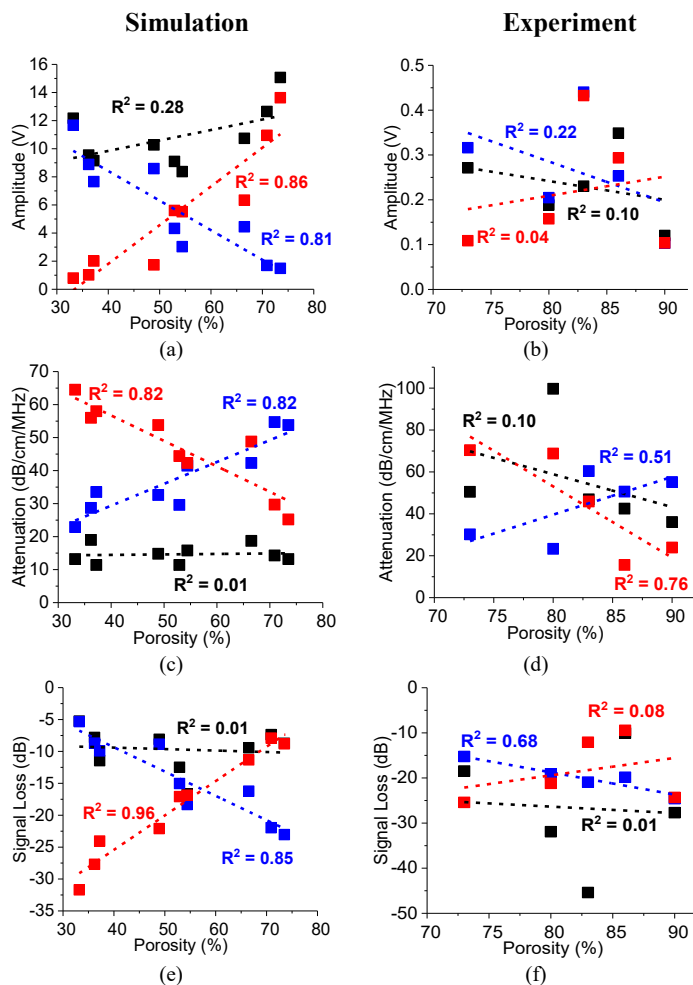$$β(f)=1/D [20 \log SB(f) − 20 \log SR(f)]\qquad(2)$$

128

Fig. 5. Graph of correlation coefficient between wave parameter with porosity. Black color represent mix wave, blue color represent fast wave and red color represent slow wave.

3 (b), the reflected slow wave arrival time was almost equal while the reflected fast wave arrival time was roughly 0.5 μs in advance compared to reference wave arrival time (i.e., time = 0 μs). The relationship in terms of arrival time for *yfast(t)* and *hfast(t)* or *yslow(t)* and *hslow(t)* can be seen in Fig. 3 (a) and (b). Another proved of the two modes waves presence can be seen based on the different oscillation frequencies between *hslow(t)* and *hfast(t)* as shown in Fig. 3 (a), where the oscillation frequency at the *hfast(t)*'s region was lower than *hslow(t)*'s region.

The difference between the oscillation frequency of the transfer function as shown in Fig. 3 (a) also supported by the centre frequency of reflected fast and slow as shown in frequency domain waveform in Fig. 4 (a), where the centre frequency of reflected slow wave, f_0Rslow (0.78 MHz) was higher than the centre frequency of reflected fast wave, f_0Rfast (0.71 MHz). Previous work by Wear [14] and Cardoso *et al.* [7] also shows the same result in terms of differences oscillation frequency between fast and slow wave. Moreover, the reflected slow wave amplitude spectrum, *ARslow* (0.29 V) was also higher than reflected fast wave amplitude spectrum, *ARfast* (0.25 V). The result is also in good agreement with previous work, where fast waves are typically lower than slow waves in amplitude [3-8]. Previous works found that high-frequency signal attenuated faster than the low-frequency signal [7, 30].

Based on this observation, because the f_0Rfast is slightly lower than f_0Rslow, the *ARfast* can be presumed to experience a slightly higher attenuation effect compared to *ARslow*. That's why *ARfast* value is a bit lower than *ARslow*. Based on these two observations (amplitude and frequency), it can be assumed that fast wave (*ARfast*) propagate through solid PU, which has slightly higher attenuation effect. Meanwhile, slow wave (*ARslow*) propagates through pore part of the porous structure.

B. Ultrasound Wave Parameter Versus Porosity

As shown in Fig. 5 (a) – *Simulation*, the reflected fast wave amplitude, *ARfast* shows decreasing trends, while both reflected mix and slow wave amplitude, *ARmix* and *ARslow* shows increasing trends versus porosity. The correlation coefficients are significant for both *ARfast* and *ARslow*, where the value is $R^2 = 0.81$ and $R^2 = 0.86$, respectively. Meanwhile, the correlation coefficient of *ARmix* versus porosity is low. Referring to Fig. 5 (b) – *Experiment*, all reflected wave amplitude (mix, fast and slow) shows low or no clear correlation versus porosity. In Fig. 5 (c) – *Simulation*, both reflected fast and slow wave attenuation, *βRfast* and *βRslow* show significant correlation versus porosity, where both values are similar ($R^2 = 0.82$). *βRfast* demonstrated increasing trends, while *βRslow* shows decreasing trends when porosity increase. However, reflected mix wave attenuation, *βRmix* shows no correlation with porosity.

Fig. 5 (d) – *Experiment* shows that, both *βRmix* and *βRslow* shows decreasing trends versus porosity. However, the correlation coefficient of *βRslow* ($R^2 = 0.75$) is higher than *βRmix* ($R^2 = 0.10$). Besides, *βRfast* shows increasing trends versus porosity with a slightly significant correlation coefficient ($R^2 = 0.51$). In Fig. 5 (e) – *Simulation*, both reflected fast and slow wave signal loss, *SLRfast* ($R^2 = 0.85$) and *SLRslow* ($R^2 = 0.96$) show significant correlation versus porosity. *SLRfast* shows an increasing trend, while *SLRslow* shows decreasing trends versus porosity. However, *SLRmix* shows low correlation versus porosity. As shown in Fig. 5 (f) – *Experiment*, *SLRfast* ($R^2 = 0.68$) shows a slightly significant correlation while both *SLRslow* and *SLRmix* shows low correlation versus porosity. *SLRfast* also shows increasing trends versus porosity.

The compactness of the solid structure will decrease as the porosity grows. Since the fast wave propagates through the solid structure, the fast wave amplitude parameters would be negatively influenced by this phenomenon. The same finding was also recorded in previous research, where the fast wave amplitude decreases as porosity increases [6, 10, 17, 31, 32]. In this study, *ARfast* for both simulation and experiment also shows decreasing trends versus porosity. However, increasing porosity will also increase the distance between pore spaces of the porous structure. This occurrence will enhance the flow of fluid [33], thereby, will increase the effectiveness of the slow wave propagation that leads to increasing amplitude parameters. Unlike fast wave, slow wave has been proved correspond to the pore part of the porous structure [6, 10, 17, 31, 32]. Nevertheless, in this analysis, only *ARslow – simulation* reveals increased trends versus porosity. The backscattered wave studied by Hosokawa [3, 16-18] also shows similar patterns in the behaviour of backscattered fast and slow wave amplitude parameters as porosity increases.

For the attenuation parameters, previously researched by Cardoso *et al.* [7] shows that, fast wave attenuation increase from low to mid porosity (50 % to 75 %). However, when the porosity level increases further from 75 % to 90 %, fast wave attenuation parameters shows decreases trends. Meanwhile, slow wave attenuation shows a slightly increases trend versus porosity and at high porosity level, both attenuations of fast and slow wave seem to converge. It's indicating that the slow wave dominated the attenuation parameter at the high porosity level. Also, Hoffman *et al.* [32] found that using Bayesian method to separate fast and slow wave, both fast and slow wave attenuation shows decreasing trends due to sonometry effect (higher density contribute to higher attenuation). In this study, *βRfast – simulation* shows increasing trends might correspond to *ARfast – simulation*, while for the *βRslow – simulation*, the decreases trends were corresponding to increases of *ARslow – simulation*. However, different behaviour occurs to the experiment result and despite the amplitude parameters shows low overall correlation coefficient, the attenuation still shows good correlation with porosity. This occurrence may be due to the calculation of the attenuation parameters, concentrating on the attenuation slope instead of the single point value of the broadband signal.

In terms of signal loss parameters, the decreases trends of *ARfast – simulation* might contribute to increases of *SLRfast – simulation* (a similar situation also occur to the *βRfast – simulation*). Meanwhile, vice versa occurs to the behaviour of *SLRslow – simulation* versus porosity. For the experiment, the overall behaviour of amplitude parameters also influences the overall signal loss parameters. However, the *SLRfast – experiment* ($R^2 = 0.68$) shows a better correlation coefficient value compared to *ARfast – experiment* ($R^2 = 0.22$). Not only that but the simulation result also in good agreement with the results, where both *SLRfast* and *SLRslow – simulation* ($R^2 = 0.85$ and 0.96) shows slightly higher correlation coefficient value compared to both *ARfast* and *ARslow – simulation* ($R^2 = 0.81$ and 0.86). Since the signal loss value is different for each frequency of the broadband signal, the measurement taken at the specific frequency i.e., the centre frequency seems to provide a better correlation with changes of porosity. Meanwhile, the amplitude parameter is taken at the max value of the frequency domain waveform without considered the frequency.

Comparison result between simulation and experiment shows that the overall results in terms of ultrasound wave correlation with porosity obtained by the simulation are better than the experiments. Several factors might contribute to the results. One of the factors is the unwanted noise interference. The experiment result might suffer from additional noise interference and because of this, the overall results of the correlation coefficient specifically amplitude and signal loss parameter is low. However, the attenuation parameters seem less affected by the noise. As mention before, the attenuation parameter calculation is focused on the slope of the attenuation instead of a single point of data might less affect by noise interference. Even though the simulation and experiment are different, especially in terms of the sample (porosity ranges, type of samples, etc.), equipment setup and others, some of the results which is attenuation parameter are in good agreement between them. Also, the value of the parameter that was set in the simulation is referenced to the acoustic properties of the PU

materials. The reason is to simulate the condition as close as possible to the condition of the experiment. The overall results also in good agreement with previous works [10], where fast wave correspond to a solid structure, while slow wave corresponds to the pore part of the porous structure. However, the result might be different if compared with real bone since the acoustic materials between bone and polyurethane are different. Nevertheless, this study shows the comparison of the performance in terms of the correlation with porosity between mix wave and two modes wave. Besides, this study also suggests the ultrasound parameters that provide the best result and less affected by noise or any unwanted interference..

IV. CONCLUSION

In conclusion, the bandlimited deconvolution approach is capable of separating and estimating the reflected fast and slow waves from the reflected mix wave obtained using the PE measurement technique. Based on the centre frequency and waveform amplitude, fast and slow wave can be identified and also predicted which wave propagates through solid or pore region. Fast wave propagates through a solid structure, while slow wave propagates through pore part of the porous structure. The overall simulation result shows that the reflected fast and slow wave parameters show a significant correlation coefficient with porosity. However, only attenuation parameters show a significant correlation with porosity for the experiment result. Additional unwanted noise might affect the experiment result, especially for the amplitude and signal loss parameters. Despite the are several differences between simulation and experiment, the attenuation result is in good agreement with each other. Overall findings indicated that considering fast and slow waves to be used to estimate bone quality could be an alternate approach and could also help to increase PE measurement accuracy.

REFERENCES

[1] V. Chijindu, C. Udeze, M. Ahaneku, and E. Anoliefo, "Detection of Prostate Cancer Using Radial/Axial Scanning of 2D Trans-rectal Ultrasound Images," *Bulletin of Electrical Engineering and Informatics,* vol. 7, pp. 222-229, 2018.

[2] A. C. Toufik Merdjana, "Study and simulation with VHDL-AMS of the electrical impedance of a piezoelectric ultrasonic transducer " *International Journal of Power Electronics and Drive System (IJPEDS),* vol. 10, pp. 1064 - 1071 June 2019 2019.

[3] A. Hosokawa, "Numerical Analysis of Ultrasound Backscattered Waves in Cancellous Bone Using a Finite-Difference Time-Domain Method: Isolation of the Backscattered Waves From Various Ranges of Bone Depths," *Ieee Transactions on Ultrasonics Ferroelectrics and Frequency Control,* vol. 62, pp. 1201-1210, Jun 2015.

[4] Y. Nagatani, V.-H. Nguyen, S. Naili, and G. Haïat, "The effect of viscoelastic absorption on the fast and slow wave modes in cancellous bone," in *6th European Symposium on Ultrasonic Characterization of Bone (ESUCB)* 2015, pp. 1-2.

[5] S. Kawasaki, R. Ueda, A. Hasegawa, A. Fujita, T. Mihata, M. Matsukawa*, et al.*, "Ultrasonic wave properties of human bone marrow in the femur and tibia," *J Acoust Soc Am,* vol. 138, pp. EL83-7, Jul 2015.

[6] T. Otani, "Quantitative estimation of bone density and bone quality using acoustic parameters of cancellous bone for fast and slow waves," *Japanese journal of applied physics,* vol. 44, p. 4578, 2005.

[7] L. Cardoso, F. Teboul, L. Sedel, C. Oddou, and A. Meunier, "In vitro acoustic waves propagation in human and bovine cancellous bone," *J Bone Miner Res,* vol. 18, pp. 1803-12, Oct 2003.

[8] A. M. Nelson, J. J. Hoffman, M. R. Holland, and J. G. Miller, "Single mode analysis appears to overestimate the attenuation of human calcaneal bone based on Bayesian-derived fast and slow wave mode analysis," in *IEEE International Ultrasonics Symposium*, 2012, pp. 1015-1018.

[9] Y. Nagatani, K. Mizuno, and M. Matsukawa, "Two-wave behavior under various conditions of transition area from cancellous bone to cortical bone," *Ultrasonics,* vol. 54, pp. 1245-1250, Jul 2014.

[10] A. Hosokawa, Y. Nagatani, and M. Matsukawa, "The Fast and Slow Wave Propagation in Cancellous Bone: Experiments and Simulations," in *Bone Quantitative Ultrasound*, ed: Springer, 2011, pp. 291-318.

[11] A. M. Groopman, J. I. Katz, M. R. Holland, F. Fujita, M. Matsukawa, K. Mizuno, *et al.*, "Conventional, Bayesian, and Modified Prony's methods for characterizing fast and slow waves in equine cancellous bone," *The Journal of the Acoustical Society of America,* vol. 138, pp. 594-604, 2015.

[12] H. Taki, Y. Nagatani, M. Matsukawa, H. Kanai, and S.-I. Izumi, "Fast decomposition of two ultrasound longitudinal waves in cancellous bone using a phase rotation parameter for bone quality assessment: Simulation study," *The Journal of the Acoustical Society of America,* vol. 142, pp. 2322-2331, 2017.

[13] M. Grimes, A. Bouhadjera, S. Haddad, and T. Benkedidah, "In vitro estimation of fast and slow wave parameters of thin trabecular bone using space-alternating generalized expectation-maximization algorithm," *Ultrasonics,* vol. 52, pp. 614-21, Jul 2012.

[14] K. A. Wear, "Time-domain separation of interfering waves in cancellous bone using bandlimited deconvolution: Simulation and phantom study," *The Journal of the Acoustical Society of America,* vol. 135, pp. 2102-2112, 2014.

[15] K. Wear, Y. Nagatani, K. Mizuno, and M. Matsukawa, "Fast and slow wave detection in bovine cancellous bone in vitro using bandlimited deconvolution and Prony's method," *The Journal of the Acoustical Society of America,* vol. 136, pp. 2015-2024, 2014.

[16] A. Hosokawa, "Numerical analysis of fast and slow waves backscattered from various depths in cancellous bone," in *Ultrasonics Symposium (IUS), 2015 IEEE International*, 2015, pp. 1-4.

[17] A. Hosokawa, "Variations in reflection properties of fast and slow longitudinal waves in cancellous bone with boundary condition," in *Ultrasonics Symposium (IUS), 2013 IEEE International*, 2013, pp. 2076-2079.

[18] A. Hosokawa, "Numerical investigation of reflection properties of fast and slow longitudinal waves in cancellous bone: Variations with boundary medium," *Japanese Journal of Applied Physics,* vol. 53, p. 07KF13, 2014.

[19] R. P. Gilbert, P. Guyenne, and J. Li, "Numerical investigation of ultrasonic attenuation through 2D trabecular bone structures reconstructed from CT scans and random realizations," *Comput Biol Med,* vol. 45, pp. 143-56, Feb 2014.

[20] M. Molero-Armenta, U. Iturrarán-Viveros, S. Aparicio, and M. Hernández, "Optimized OpenCL implementation of the elastodynamic finite integration technique for viscoelastic media," *Computer Physics Communications,* vol. 185, pp. 2683-2696, 2014.

[21] Signal-Processing. (8 July 2019). *Ultrasonic or ultrasound sound velocity and impedance*. Available: https://www.signal-processing.com/table.php.

[22] V. Shim, J. Boheme, C. Josten, and I. Anderson, "Use of polyurethane foam in orthopaedic biomechanical experimentation and simulation," in *Polyurethane*, ed: InTech, 2012.

[23] S. Worldwide, "Biomechanical Test Materials Catalogue," *Vashon, WA*.

[24] P. Laugier and G. Haïat, *Bone quantitative ultrasound* vol. 576: Springer, 2011.

[25] K. R. Marutyan, G. L. Bretthorst, and J. G. Miller, "Bayesian estimation of the underlying bone properties from mixed fast and slow mode ultrasonic signals," *The Journal of the Acoustical Society of America,* vol. 121, pp. EL8-EL15, 2007.

[26] K. R. Marutyan, M. R. Holland, and J. G. Miller, "Anomalous negative dispersion in bone can result from the interference of fast and slow waves," *The Journal of the Acoustical Society of America,* vol. 120, pp. EL55-EL61, 2006.

[27] M. A. Abd Wahab, R. Sudirman, M. A. A. Razak, F. K. C. Harun, and N. A. A. Kadir, "Comparison of Fast and Slow Wave Correlation with Various Porosities between Two Measurement Technique," in *2019 IEEE Student Conference on Research and Development (SCOReD)*, 2019, pp. 39-44.

[28] M. A. Abd Wahab, R. Sudirman, M. A. A. Razak, F. K. C. Harun, N. A. A. Kadir, and N. H. Mahmood, "Incident and reflected two waves correlation with cancellous bone structure," *TELKOMNIKA,* vol. 18, pp. 1968-1975, 2020.

[29] M. Salim, M. Ahmmad, S. Rosidi, B. Ariffin, I. Ahmad, and A. Supriyanto, "E. Measurements of Ultrasound Attenuation for normal and pathological mice breast tissue Using 10MHz Ultrasound Wave," in *Proceeding of The 3rd WSEAS International Conference on Visualization, Imaging and Simulation*, 2010.

[30] K. A. Wear, "Ultrasonic scattering from cancellous bone: a review," *IEEE transactions on ultrasonics, ferroelectrics, and frequency control,* vol. 55, pp. 1432-1441, 2008.

[31] F. Meziere, M. Muller, E. Bossy, and A. Derode, "Measurements of ultrasound velocity and attenuation in numerical anisotropic porous media compared to Biot's and multiple scattering models," *Ultrasonics,* vol. 54, pp. 1146-54, Jul 2014.

[32] J. J. Hoffman, A. M. Nelson, M. R. Holland, and J. G. Miller, "Cancellous bone fast and slow waves obtained with Bayesian probability theory correlate with porosity from computed tomography," *The Journal of the Acoustical Society of America,* vol. 132, pp. 1830-1837, 2012.

[33] K. I. Lee, "Relationships of linear and nonlinear ultrasound parameters with porosity and trabecular spacing in trabecular-bone-mimicking phantoms," *The Journal of the Acoustical Society of America,* vol. 140, pp. EL528-EL533, 2016.